

Preparation of a Novel Copper Catalyst in Terms of the Immiscible Interaction Between Copper and Chromium

Satoshi Kameoka · Mika Okada · An Pang Tsai

Received: 19 April 2007 / Accepted: 10 September 2007 / Published online: 29 September 2007
© Springer Science+Business Media, LLC 2007

Abstract Based on the metallurgical point of view, we aimed to design a new form of copper catalysts with high thermal stability and activity. Delafossite CuCrO_2 has been studied as a precursor for copper catalyst. The CuCrO_2 was reduced to fine dispersion of Cu and Cr_2O_3 particles with porous structure by the treatment in H_2 at 600 °C, which exhibited much higher activity and thermal stability for steam reforming of methanol (SRM) than those of the CuO and/or Cr_2O_3 catalysts. Sintering of Cu particles was significantly suppressed even after H_2 reduction at 600 °C. Moreover, the CuCrO_2 can be regenerated by calcination in air at 1,000 °C where the activity is also restored completely even after sintering at high temperatures. Fine porous structure generated by the reduction of CuCrO_2 and immiscible interaction between Cu and Cr_2O_3 are important in stabilizing of copper nanoparticles. Based on these findings, we propose that the CuCrO_2 is an effective precursor for a high performance copper catalyst.

Keywords CuCrO_2 · Delafossite · Immiscible · Porous structure · Thermal stability · Reversible · Methanol steam reforming

1 Introduction

Copper-based catalysts are extensively studied due to their good catalytic performance in several reactions such

as steam reforming of methanol and water gas shift reaction [1, 2]. Difficulty of homogeneous dispersion of Cu particles on supports and poor thermal stability have been the major drawbacks [3]. To overcome these problems, catalytic performance of copper-based catalysts has been improved by combination with the metal oxides such as ZnO [3–5], Cr_2O_3 [5, 6], Fe_2O_3 [7, 8], and CoO [9]. However, roles of the oxides in the improved copper-based catalysts have not been sufficiently understood. According to the binary alloy equilibrium phase diagrams, Cu and M (M = Fe, Cr, Co, etc.) are neither form compounds nor mutually dissolve in the solid state, i.e., Cu and M are immiscible [10]. Recently, we have found that copper catalysts with fine dispersion of copper particles and high thermal stability can be directly prepared from a spinel CuFe_2O_4 in which the combination of Cu with Fe is important [7, 11]. High catalytic performance is ascribed to the reduction of the spinel CuFe_2O_4 and the subsequent immiscible interaction between Cu and Fe [7]. The origin of high catalytic performance is due to the formation of a composite structure induced by reductive decomposition of the CuFe_2O_4 where nano-scale copper particles homogeneously dispersed within the porous Fe_3O_4 matrix [11]. With understanding of interaction between the constituent metals in mixed oxides, one may logically design a promising catalyst. In this material design, metallurgical background is very helpful.

Based on the metallurgical point of view, we have investigated a process for preparation of a new form of copper catalysts with high catalytic performance. In this work, we examine the morphological change before and after reduction and the regeneration of the delafossite CuCrO_2 in the redox treatments and claim the role of the interaction of chromium (or chromium oxides) with copper in the CuCrO_2 .

S. Kameoka (✉) · M. Okada · A. P. Tsai
Institute of Multidisciplinary Research for Advanced Materials,
Tohoku University, 2-1-1 Katahira, Aoba-ku, Sendai 980-8577,
Japan
e-mail: kameoka@tagen.tohoku.ac.jp

2 Experimental

The CuCrO_2 catalyst was prepared by the following method. Stoichiometric mixtures (atomic ratio $\text{Cu/Cr} = 1$) of high purity CuO (NanoTek, C.I. Kasei Co.) and Cr_2O_3 (Wako Pure Chemical Industries, Ltd.) powders were homogenized in an agate mortar. The mixed powder was calcined in air at $1,000^\circ\text{C}$ for 12 h and cooled down slowly. For comparison, CuO and $\text{CuO} + \text{Cr}_2\text{O}_3$ (physical mixture) catalyst were also studied. The steam reforming of methanol (SRM) experiments were carried out in a conventional flow reactor at 100 kPa. Inlet partial pressure of methanol, water and nitrogen were 35.5, 52.7, and 13.2 kPa, respectively (LHSV of $\text{CH}_3\text{OH}/\text{H}_2\text{O}$ mixture: 30 h^{-1}). Here nitrogen was used as diluent. All samples were pretreated with H_2 at 460 or 600°C for 1 h in a flow reactor before reaction. The products were analyzed by an on-line gas chromatograph (Shimadzu GC 14A) equipped with Shincarbon column (H_2 , CO , CO_2 , and CH_4) under Ar carrier gas. The catalytic activity for the SRM was evaluated by the H_2 production rate ($\text{mL STP min}^{-1}\text{ g-cat}^{-1}$). The data in the catalytic activity measurements were recorded when the reaction reached steady state after 30 min. The turnover frequencies (TOFs) were calculated by dividing the H_2 production rate by the total amount of surface copper atoms. The total amount of the surface copper metal sites was estimated by oxygen adsorption on reduced Cu via N_2O decomposition at 90°C : $\text{N}_2\text{O} + 2\text{Cu}_s^0 \rightarrow \text{Cu}_2\text{O} + \text{N}_2 \uparrow$ where Cu_s is a surface Cu atom [12]. Surface area determination of particle was made by BET analysis. Pore structure and pore size distributions of the samples were obtained from N_2 adsorption–desorption isotherms at -196°C . The phase identification of each sample was performed by X-ray diffraction (Mac science M03XHF22) using $\text{Cu K}\alpha$ ($\lambda = 1.543\text{ \AA}$) radiation. The copper crystallite sizes of the samples were estimated from the XRD line broadening analysis using the Scherrer equation for the $\text{Cu}(111)$ reflection. The H_2 –TPR measurements were carried out using 50 mg of the catalyst from room temperature to 600°C at a heating rate of 4°C/min in 5% H_2/Ar flow (30 mL/min). The surfaces of the samples were observed by a scanning electron microscopy (LEO 982).

3 Results and Discussion

Figure 1 shows the XRD patterns of CuCrO_2 catalyst before and after H_2 reduction treatment. As shown in Fig. 1, the peaks responsible for delafossite CuCrO_2 were observed before H_2 reduction [13]. It is noted that a single phase of the delafossite CuCrO_2 was formed in the mixture of CuO and Cr_2O_3 calcined in air at $1,000^\circ\text{C}$ [13, 14]. Figure 2 shows the H_2 –TPR profile of the CuCrO_2 catalyst.

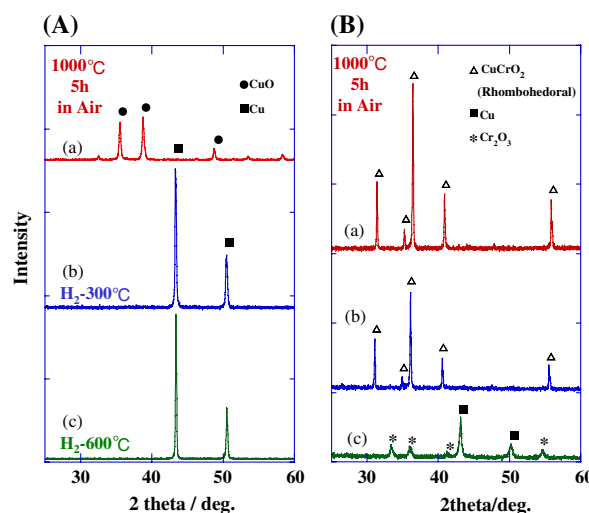


Fig. 1 Powder X-ray diffraction patterns of the CuO (A) and the CuCrO_2 (B) as a function of H_2 reduction temperature: (a) before, (b) 460°C , and (c) 600°C

As shown in Fig. 2, a peak responsible for reduction around 670°C is observed for the CuCrO_2 catalyst, which is attributed to the reduction of CuCrO_2 to Cu and Cr_2O_3 . The changes in XRD patterns along the reduction temperature are in good consistent with the TPR profile for the CuCrO_2 catalyst. The XRD patterns and the H_2 –TPR profile of CuO are also shown in Figs. 1 and 2 for comparison. As shown in Fig. 1, after the H_2 reduction, the diffraction peaks of Cu are very sharp when the precursor is CuO , while those are much broadening when the precursor is CuCrO_2 , indicating that sintering of Cu particles generated from the CuCrO_2 has been significantly suppressed by the presence of chromium even after the H_2 reduction at high temperatures ($\sim 600^\circ\text{C}$).

Table 1 summarized the results of the BET surface area measurement. It is clear that the surface area of the CuCrO_2 increases by one order after H_2 reduction at 600°C . In contrast, the surface areas of the CuO and the $\text{CuO} + \text{Cr}_2\text{O}_3$ catalysts drastically decrease after the H_2 reduction treatments. Figure 3 shows the pore size distribution estimated from the BET measurement before and after H_2 reduction for the CuCrO_2 . After H_2 reduction at 600°C , the CuCrO_2 catalyst showed the broad pore size distribution with a peak around 7 nm, indicating that the observed increase in surface area is due to formation of these fine meso-pores. For the CuO and the $\text{CuO} + \text{Cr}_2\text{O}_3$ catalysts after H_2 reduction, the surface areas are smaller than $0.05\text{ m}^2/\text{g}$ for the CuO and $1.1\text{ m}^2/\text{g}$ for the $\text{CuO} + \text{Cr}_2\text{O}_3$, respectively, which are much smaller than that of the CuCrO_2 catalyst. This is ascribed to the fact that the copper particles readily aggregate during H_2 reduction at high temperatures. Figure 4 shows the SEM micrographs of the CuCrO_2 catalyst before and after H_2 reduction treatments.

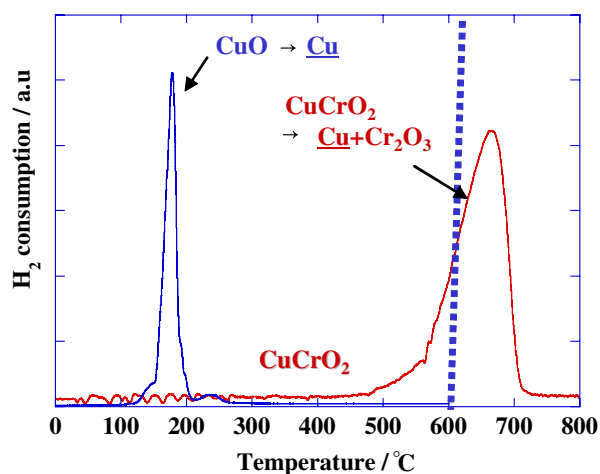


Fig. 2 H₂-TPR profiles of the CuO and the CuCrO₂ powders. TPR conditions: heating at 4 °C/min in 5% H₂/Ar

The CuCrO₂ surface was smooth before H₂ reduction, whereas precipitates came up on the surface after H₂ reduction at 460 °C. The precipitates are attributed to composite products, i.e., Cu + Cr₂O₃, by reductive decomposition of outmost surface of CuCrO₂ bulk. After H₂ reduction at 600 °C, the CuCrO₂ completely decomposed to copper and chromium oxide as verified by the XRD measurement. It should be noted that the Cr₂O₃ reveals very fine porosity, which is responsible to the high surface area and mesopore obtained by BET measurements. This indicates that the formation of mesopore was achieved by reductive decomposition of the CuCrO₂.

Figure 5 shows the rate of H₂ production as a function of reaction temperature in the SRM over the CuCrO₂, the CuO and the CuO + Cr₂O₃ catalysts after H₂ reduction at 600 °C. The CuCrO₂ catalyst significantly exhibited much higher catalytic activity than the CuO and the CuO + Cr₂O₃ catalysts. The catalytic activity of the CuCrO₂ catalyst treated at 460 °C in H₂ was very low due to insufficient reduction for the CuCrO₂ (not shown). As

Table 1 Results of BET surface area measurements (m²/g), crystallite sizes (nm), and TOF values (s⁻¹)

Catalyst	Before ^a (m ² /g)	After H ₂ reduction ^b (m ² /g)	Crystallite size ^c (nm)	TOF ^d (10 ⁻¹ s ⁻¹)
CuO	10.8	<0.05	56	0.1
CuO + Cr ₂ O ₃ (Cu/Cr = 1)	7.0	1.1	29	2.0
CuCrO ₂	0.2	2.7	17	26.0

^a Before H₂ reduction

^b After H₂ reduction at 600 °C for 1 h

^c Calculated from the XRD patterns after H₂ reduction at 600 °C using the Scherrer equation for the Cu(111) reflection

^d Reaction temperature at 280 °C

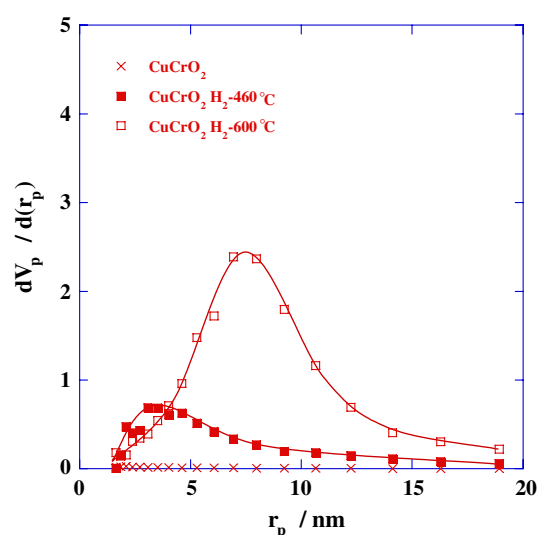


Fig. 3 Pore distribution in the CuCrO₂ powders before and after H₂ reduction: (x) before, (■) at 460 °C, and (□) at 600 °C

shown in Table 1, the TOF value of the CuCrO₂ catalyst is more than 30 and 10 times higher than those of the CuO and the CuO + Cr₂O₃ catalysts, respectively. Decrease of surface area and sharpening of diffraction peaks of copper in the CuO and the CuO + Cr₂O₃ catalysts were observed after H₂ reduction at 600 °C, indicating that sintering of copper particles readily proceed during reduction. On the other hand, the copper particles generated from the CuCrO₂ showed high catalytic activity and thermal stability. The fine porous structure forms by H₂ reduction of the CuCrO₂, which leads to the increase in the effective surface area of copper responsible for catalytic reaction.

For comparison, it is of interesting to examine reduction behavior and catalytic activity of spinel CuCr₂O₄ as a copper chromite related compound. Although the CuCr₂O₄ was not active for the SRM reaction (without H₂ reduction treatment), the catalytic activity of the CuCr₂O₄ exhibited almost comparable activity to the CuCrO₂ after the H₂ reduction at 600 °C for 1 h (not shown). The reduction of the CuCr₂O₄ during the H₂ treatment proceeds as follows: CuCr₂O₄ → (CuCrO₂ + Cu + Cr₂O₃) → Cu + Cr₂O₃, which have been reported by several research groups [15–17]. This is suggested that reduction of both the CuCr₂O₄ and the CuCrO₂ leads to form similar composite phases (Cu + Cr₂O₃) after the H₂ pretreatment at 600 °C.

In this study, we have shown a copper catalyst with high thermal stability and revealing high catalytic activity developed from the CuCrO₂. The origin of high activity and high thermal stability is the formation of a porosity structure generated by reduction of the CuCrO₂ where nano-scale Cu particles homogenously dispersed within the porous Cr₂O₃ (i.e., fine dispersion of copper particles). Remarkable increase in surface area after H₂ reduction at 600 °C is clearly derived from the formation of the porous

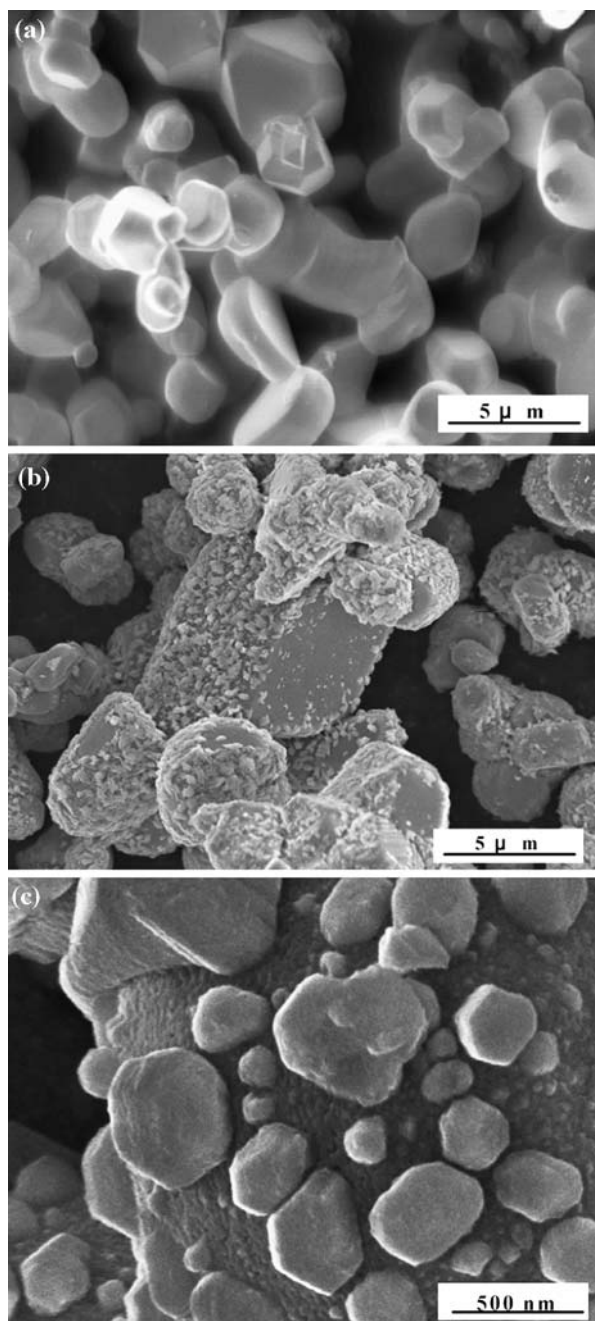


Fig. 4 SEM images for the CuCrO_2 : (a) before and after H_2 reduction treatment, (b) at 460 °C, and (c) at 600 °C

structure. Undoubtedly, the high catalytic activity is attributed to the spontaneous formation of fine copper particles dispersed in the porous chromium oxide. On the other hand, it is known in phase diagram that Cu and Cr are mutually immiscible [10], and the phase separation between copper and chromium oxide at nano-scale could keep high dispersion and high thermal stability of Cu particles.

In the H_2 -TPR and the XRD measurements, it is clear that the CuCrO_2 is reduced to Cu^* (fine dispersion of

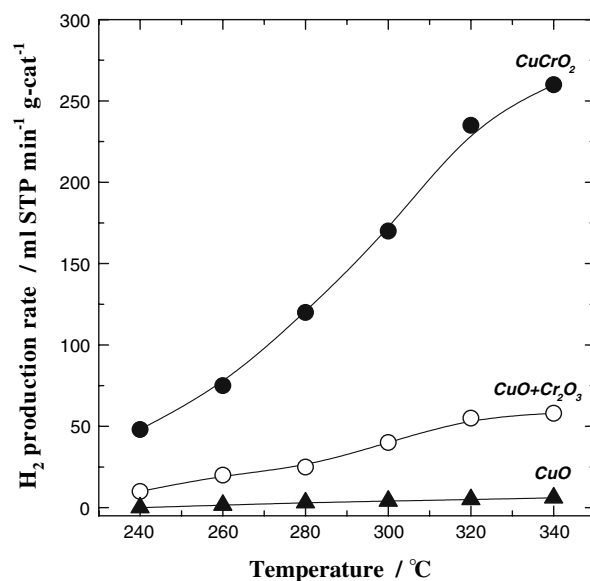


Fig. 5 The rate of H_2 production versus reaction temperatures in the steam reforming of methanol for the CuO , the $(\text{CuO} + \text{Cr}_2\text{O}_3)$ and the CuCrO_2 powders after H_2 reduction at 600 °C

copper nanoparticles) and Cr_2O_3 particles around 600 °C (Eq. (1)). Fine dispersion of copper nanoparticles is attainable by the H_2 reduction of the CuCrO_2 . These properties are ascribed to the selective reduction of the CuCrO_2 and the subsequent immiscible interaction between copper and chromium (or chromium oxides). Interestingly, the CuCrO_2 can be regenerated by treatment in air at 1,000 °C even if an intentional sintering of copper particles occurs (i.e., reversible process).



In general, due to the immiscibility of copper with chromium nanostructure with Cu and Cr cannot be obtained by conventional alloying processes such as arc melting [10]. However, Cu and Cr atoms distribute homogeneously at atomic scale in a composite oxide. Composite oxides in this case act as precursors in which Cu nanoparticles are readily formed by the H_2 reduction. In this study, we propose a simple process to design a new copper catalyst based on the concept described above. Change in the morphology of the CuCrO_2 under the redox condition deserves further attention to expand into more detailed studies including the formation of the porous structure from the CuCrO_2 and its mechanism.

4 Conclusions

The present study demonstrates the validity of delafossite CuCrO_2 as a precursor for a high catalytic performance copper catalyst. The structure consisting of fine dispersion

of Cu particles within the porous chromium oxides was obtained by the H_2 reduction at 600 °C for the CuCrO_2 , reveals high surface area and catalytic activity for SRM. The high thermal stability is ascribed to the formation of the porous structure and the subsequent immiscible interaction between Cu and Cr_2O_3 . Additionally, the delafossite CuCrO_2 was readily regenerated by calcination in air at 1,000 °C.

References

1. Takezawa N, Iwasa N (1997) *Catal Today* 36:45 and references therein
2. Newsome DS (1980) *Catal Rev Sci Eng* 21:275
3. Twigg MV, Spencer MS (2003) *Top Catal* 22:191
4. Klier K (1982) *Adv Catal* 31:243
5. Ma L, Trimm DL, Wainwright MS (1999) *Top Catal* 8:271
6. Laine J, Ferrer Z, Labady M, Chang V, Frias P (1988) *Appl Catal* 44:11
7. Kameoka S, Tanabe T, Tsai AP (2005) *Catal Lett* 100:89
8. Chen CS, Cheng WH, Lin SS (2004) *Appl Catal A* 257:97
9. Huang X, Ma L, Wainwright MS (2004) *Appl Catal A* 257:235
10. Massalski TB (ed) (1990), *Binary alloy phase diagrams*, 2nd edn, vol 2. ASM International, USA, p 1181, 1266, 1408
11. Kameoka S, Okada M, Tsai AP (2006) *Catal Catal (Shokubai)* 48:74
12. Evans JW, Wainwright MS, Bridgewater AJ, Young DJ (1983) *Appl Catal* 7:75
13. Dannhauser W, Vaughan PA (1954) *J Am Chem Soc* 77:896
14. Christopher J, Swamy CS (1992) *J Mater Sci* 27:1353
15. Tonner SP, Wainwright MS, Trimm DL, Cant NW (1984) *Appl Catal* 11:93
16. Castiglioni GL, Vaccari A, Fierro G, Inversi M, Jacono MK, Minelli G, Pettiti I, Porta P, Gazzano M (1995) *Appl Catal A* 123:123
17. Monnier JR, Hanrahan MJ, Apai G (1985) *J Catal* 92:119